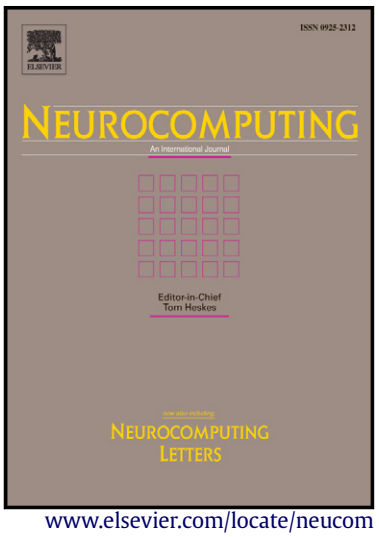

www.elsevier.com/locate/neucom

Modeling the role of fixational eye movements in real-world scenes

Andrés Olmedo-Payá, Antonio Martínez-Álvarez, Sergio Cuenca-Asensi, J.M. Ferrández, E. Fernández

PII: S0925-2312(14)01307-1
DOI: http://dx.doi.org/10.1016/j.neucom.2014.09.068
Reference: NEUCOM14751

To appear in: *Neurocomputing*

Received date: 13 June 2014
Revised date: 26 September 2014
Accepted date: 28 September 2014

Cite this article as: Andrés Olmedo-Payá, Antonio Martínez-Álvarez, Sergio Cuenca-Asensi, J.M. Ferrández, E. Fernández, Modeling the role of fixational eye movements in real-world scenes, *Neurocomputing*, http://dx.doi.org/10.1016/j.neucom.2014.09.068

Modeling the role of fixational eye movements in real-world scenes

Andrés Olmedo-Payá[a], Antonio Martínez-Álvarez[b,*], Sergio Cuenca-Asensi[b], J. M. Ferrández[c], E. Fernández[a]

[a] *Institute of Bioengineering and CIBER BBN, University Miguel Hernández, Alicante, Spain*
[b] *Department of Computer Technology, University of Alicante, Spain*
[c] *Department of Electronics and Computer Technology, Technical University of Cartagena, Spain*

Abstract

Our eyes never remain still. Even when we stare at a fixed point, small involuntary movements take place in our eyes in an imperceptible manner. Researchers agree on the presence of three main contributions to eye movements when we fix the gaze: *microsaccades*, *drifts* and *tremor*. These small movements carry the image across the retina stimulating the photoreceptors and thus avoiding fading. Nowadays it is commonly accepted that these movements can improve the discrimination performance of the retina. In this paper, several retina models with and without fixational eye movements were implemented by mean of *RetinaStudio* tool to test the feasability of these models to be incorporated in future neuroprostheses. For this purpose each retina model has been stimulated with natural scenes images in two experiments. Results are discussed from the point of view of a neuroprosthesis development.

Keywords: Fixational eye movements, microsaccades, retina simulation, spiking neurons

*Corresponding author
Email address: amartinez@dtic.ua.es (Antonio Martínez-Álvarez)

1. Introduction

Our eyes are always in constant motion. Some of these movements are involuntary and appear even when we fix our gaze. Although some of them are relatively large and displace the image across the retinal photoreceptors, they are not perceptible to us [1]. Since the late 1800s, several research groups have been investigating in understanding the role of these fixational eye movements in the vision [2] using a variety of techniques for recording [3]. Nowadays, the most accepted idea about the role of these movements is that they can improve discrimination performance in ways not explicable just by prevention of visual fading [4] [5] [6] [7]. In particular, *microsaccades* are probably the eye movements with the greatest potential to perform this task [8] [9] [10].

Various approaches have been proposed to study fixational movements. On one hand, Ditchburn et al. [11], Nachmias et al. [12] and others used recording techniques to proof the role of these eye movements in visual perception. On the other hand, simulation of *microsaccades* were used to asses in a realistic manner the role of eye movements in the primary retinal responses. Greschner et al. [13] in their work, performed an experiment which demonstrated that the simulated small movements, like *tremor*, in a turtle retina, activated sets of retinal ganglion cells in a synchronized manner. Finally, the approach based on retina models has several advantages from the point of view of experimentation. Comparing to an *in vivo* experimental setup, retina models can be easily modified and used as often as desired without the need of laboratory animals or annoying human testing. Moreover, retina models increase the range of possibilities, allowing for example, the description of diseased retinas, different isolated properties and more features that could not be done with biological retinas. In this way Donner and Hemilä [14] attempted to clarify the effects of these movements on the messages that retinal cells send to the brain by mean of mathematical models. Also, it is remarkable the work by Wohrer et al. [15] and A. Martínez et al. [16], focused primarly on the development and implementation of new retina models.

Our group is working on the development of a cortical visual neuroprosthesis aimed to restore some functional vision to profoundly visual-impaired people. For this purpose, the objective of the current study is to test the feasibility of fixational eye movements to be implemented in a visual neuroprosthesis. In this way, different retina models with and without fixational eye movements have been described and tested to check the vision improve-

ment. Results show that retina models including eye movements have a better behavior than models without this feature.

2. Retina model

The retina plays an important role in visual perception of humans. It is responsible for converting the outside world images into electrical signals understandable by the visual cortex of the brain. In fact, it is considered as a part of the brain. This process must be unequivocal and fast enough to ensure recognition of objects within a few milliseconds [17]. Therefore a good retina model, as well as its physical implementation, should take into account this time constraint to be able to respond to stimuli in real time.

In this paper several retina models which are sensitive to variations in luminance are described by mean of *RetinaStudio* [18], a framework to encode visual information that allows the specification, testing, simulation, validation and implementation of bioinspired retina models. Each retina model is defined as a matrix of different kind of ganglion cells. Models of *On* ganglion cells and *Off* ganglion cells, with and without fixational eye movements are described making a total of four different retina models: *On* model, *On + eye movements* model, *Off* model and *Off + eye movements* model.

RetinaStudio allows us to describe the different stages that comprises a biological retina. The first stage, inspired in the *Outer Plexiform Layer* of the retina was modeled by splitting the incoming images into three color channels (R,G and B). The second stage, inspired in the *Inner Plexiform Layer*, was modeled by means of spatial filters. More specifically, with a network of the well known *Difference of Gaussian* (*DoG*) filter, where σ_1 and σ_2 take the values 0.9 and 1.2 respectively in the *On* retina models and take 1.2 and 0.9 values in *Off* retina models (see equation 1).

$$DoG(x, y, \sigma_1, \sigma_2) = \frac{1}{\sqrt{2\pi\sigma_1^2}} e^{-\frac{x^2+y^2}{2\sigma_1^2}} - \frac{1}{\sqrt{2\pi\sigma_2^2}} e^{-\frac{x^2+y^2}{2\sigma_2^2}} \quad (1)$$

The magnitude value of these parameters have already been studied in the work of Morillas et al. [19]. The *Difference of Gaussian* filter receives contributions of the three types of photoreceptors R, G and B (for red, green and blue), and thus generates a *mexican-hat* contribution for every color

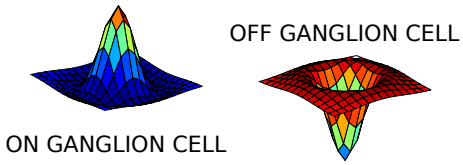

Figure 1: Center-periphery behavior of *On* and *Off* receptive fields.

channel. This contribution simulates the circular shape and the antagonist center-periphery behavior of the receptive fields of ganglion cells in the retina, see Fig. 1. Finally, inspired in the Ganglion Cell Layer, the *Leakage-Integrate&Fire* spiking neuron model proposed by Gerstner and Kistler [20] is used to model the ganglion cell firing behavior.

All retina models represent a piece of fovea having a size of 1.8×1.8 mm, where each receptive field is about $180\mu m$ of diameter [21].

2.1. Eye movements

The three main contributions of involuntary eye movements were integrated within our retina models: *tremor*, *drifts* and *microsaccades*.

2.1.1. Tremor

Tremor is the amplitude-smallest of all eye movements. It consists in an aperiodic oscillation of the eyes with small amplitudes and frequencies within the range of the recording system noise [22]. Following the work of Ratliff and Riggs [3], these movements are described in our model as oscillatory waves with an small amplitude. More specifically the amplitude is in the range between $2{,}83\mu m$ and $4{,}13\mu m$, and the frequency is 50Hz. The generated oscillatory waves are superimposed on *drifts*, see Fig. 2.

2.1.2. Drifts

Drifts are slow curvy motion that occurs between *microsaccades* and appear simultaneously with *tremor*. This movement can displace the image across a dozen photoreceptors with a mean speed of 6 arcminute/s [2]. *Drifts* are described using the *gamma* distribution of equation 2 as proposed by [23]. In our case, $\lambda = 1$ and different k values are randomly chosen taking integer values between 1 and 9. The angle of these *drifts* is randomly modified using equations 3, taken into account that all *drifts* must be directed outwards [24].

$$f(x) = \lambda e^{-\lambda x} \frac{(\lambda x)^{k-1}}{(k-1)!} \quad (2)$$

$$\begin{aligned} x' &= xcos(\theta) - ysin(\theta) \\ y' &= xsin(\theta) + ycos(\theta) \end{aligned} \quad (3)$$

In our model each drift movement have a duration between $0.24s$ and $0.48s$, with a mean of $0.36s$, and an amplitude between $68\mu m$ and $100\mu m$, with a mean of $84\mu m$. The values of duration and amplitude were randomly chosen within these ranges.

2.1.3. Microsaccades

Microsaccades are fast eye movements of short duration, about $25ms$ [4], displacing the image across a range of several dozen to several hundred photoreceptors widths. The role of *microsaccades* in visual perception have been debated for years. The most accepted idea is that its main role is to prevent fading and thus keep the vision [11] [12].

All *microsaccades* are modeled in our retina model as rectilinear movements directed to the center of the visual scene and appearing just after *drifts* with a random angle and amplitude. The amplitude of each *microsaccade* have a mean of $100\mu m$ and a duration of $20ms$. Fig. 2 shows an example of fixational eye movements paths. As can be seen, high-frequency oscillatory paths (*tremor*) are superimposed on *drifts* (curved lines) forming only one path moving slowly. *Microsaccades* (rectilinear lines) appear just after *drifts* and move the image across the retina quickly.

3. Experiments and Results

To assess the role and behavior of *microsaccades* and the other small eye movements in the perception of natural scenes, two experiments have been designed involving different retina models.

The first experiment analyze the behavior of four retina models with and without eye movements (*On*, *On + eye movements*, *Off* and *Off + eye movements*) when it is exposed to a natural scene in movement. The second experiment analyze the behavior of the same retina models when it is exposed to a static natural scene, simulating the fixational gaze.

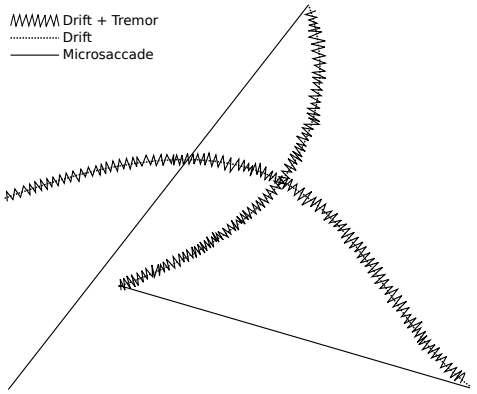

Figure 2: *Microsaccades*, *drifts* and *tremor* movements. Continuous line shows the fast *microsaccade* movement. Dashed line shows the slow curve of *drifts* movements. Oscillatory line shows the combination of *drifts* and *tremor*.

In both experiments we attempt to demonstrate the importance of these small movements in contour discrimination of natural scenes.

3.1. Natural scenes in movement

For the first experiment each retina model is defined as a 10×10 matrix of different kind of ganglion cells following the work of Ferrandez et al. [25] which uses a *Utah Electrode Array* [26] to perform extracellular recordings.

Each retina model was stimulated using a stimulus of 8,5 seconds of duration taken from a video file. The stimulus has a framerate of 25 fps with a resolution of 622×622 pixels and 8-bits of color depth (gray-scale). The video was created using *Visionegg* [27]. The records were generated in *Neural Events File* format [28] and processed with *NeurALC* [29]. This test was repeated 10 times.

Top plot in the Fig. 3 shows the whole natural scene, where a superimposed black rectangle indicates the image area stimulating our retina model at a given time. This rectangle travels across the image from left to right during the stimulation. As a measure of retinal activity it was considered the *gray mean value* [30] (equation 4), represented in the plot as color-pale graphic and calculated from the natural scene as:

$$M(x) \quad = \quad \frac{1}{m}\sum_{y=1}^{m}(x,y) \tag{4}$$

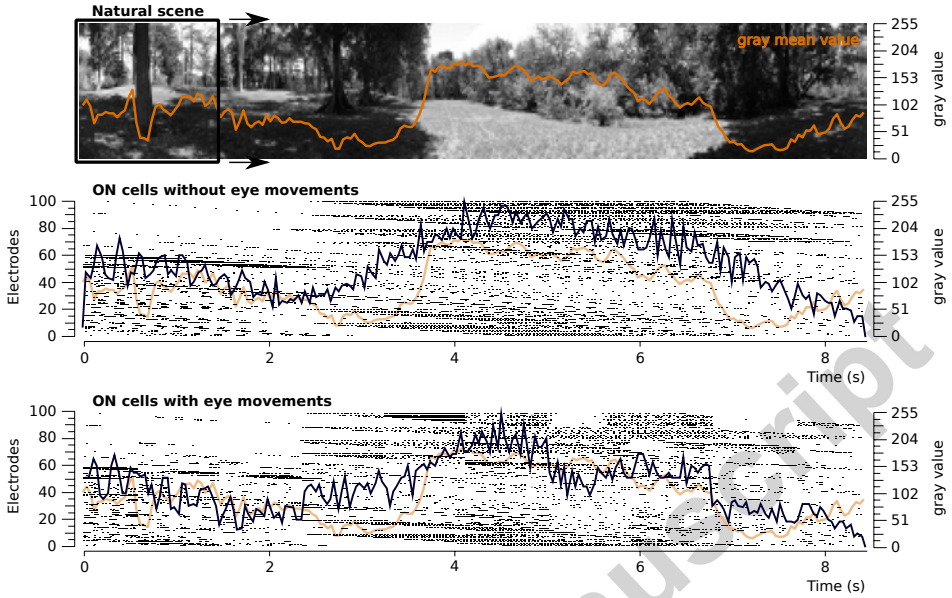

Figure 3: Raster plot showing the spike trains produced for 100 electrodes and the *population activity* with a bin of $40ms$ for *On* cells.

where $n \times m$ is the image resolution and (x, y) represent the value of a pixel.

Middle and bottom plots show, with black points, the spike trains produced by 100 electrodes in a raster plot. The *population activity* graphic is represented by a dark line and the *gray value mean* is superimposed in both plots for comparison purposes.

By inspecting the figure, it can be observed that the activity is greater in lighter areas of the exposed image and lower in the dark ones as expected. The electrodes located on the lighter areas have greater activity than those located in other areas (see raster plot). Moreover, the *population activity* graphic is more similar to *gray value mean* graphic in the retina model with eye movements implemented than those without them. It should be noted that the *population activity* have been normalized to values between 0 and 255 for comparison.

Fig. 4 shows the *population activity* for the *Off* retina model compared with the complementary *gray value mean* (see equation 5).

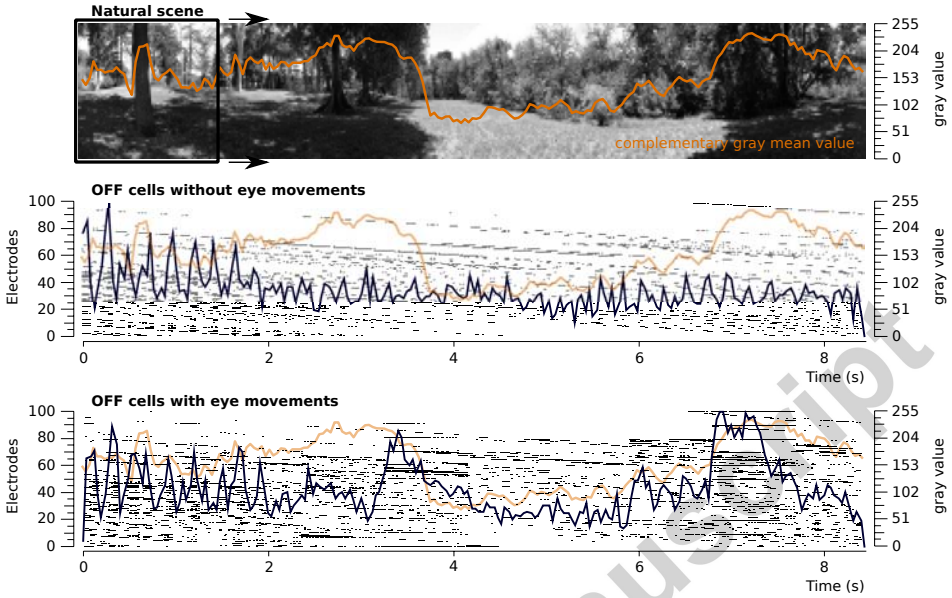

Figure 4: Raster plot showing the spike trains produced for 100 electrodes and the *population activity* with a bin of $40ms$ for *Off* cells.

$$M'(x) = 255 - \frac{1}{m}\sum_{y=1}^{m}(x,y) \tag{5}$$

In this case, unlike Fig. 3, the activity is greater in dark areas of the exposed image and lower in the lighter ones. When comparing with the *population activity*, it is clear that both signals are closer when eye movements are applied.

To measure how different is the *population activity* of our models when applying or not eye movements, a similarity measure based on a subtraction was performed between *gray value mean* graphic and *population activity* graphic. It is showed in equation 6,

$$S_{12} = \frac{1}{N}\sum_{n=1}^{N}(x_1[n] - x_2[n])^2 \tag{6}$$

where $x_1[n]$ and $x_2[n]$ corresponds to *gray value mean* and *population activity* respectively.

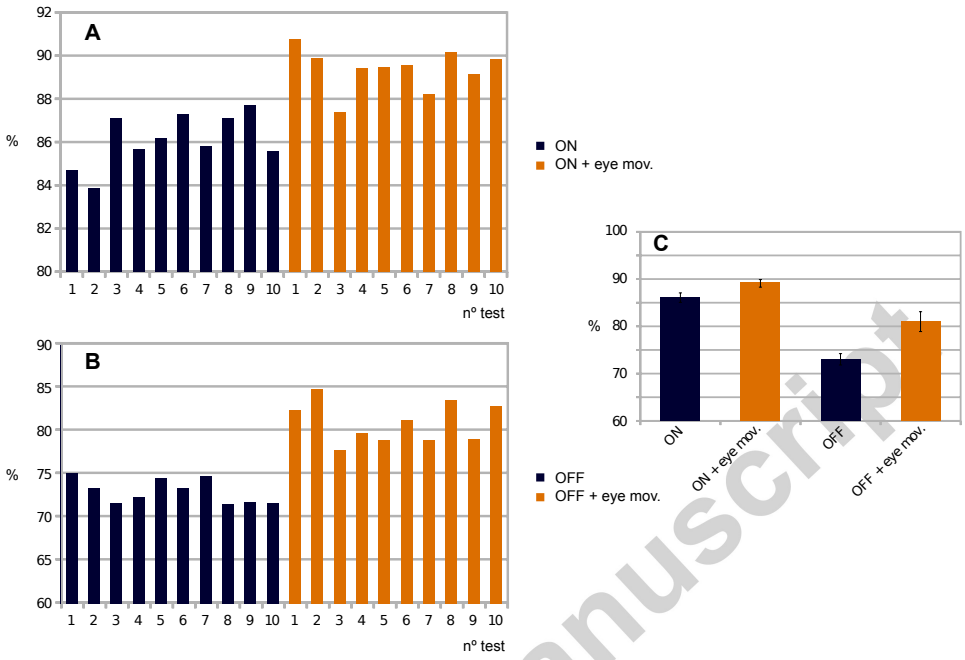

Figure 5: Percent similarity between *population activity* and *gray value mean*. Pale and dark bars represent models with and without eye movements respectively: **A** Similarity in ten simulations for *On* model. **B** Similarity in ten simulations for *Off* model. **C** Average of ten simulation for *On* model and *Off* model.

The similarity measure provided by this subtraction is depicted in Fig. 5, where the 100% corresponds with identical response in the *gray value mean* and the retina model ($S_{12} = 0$ in equation 6). Plots **A** and **B** show the similarity of ten simulations of the four retina models, plot **C** shows the average of ten simulations. Pale and dark bars represent retina models with and without eye movements respectively.

As can be seen, there is a remarkable difference between dark bars and pale bars, being the pale bars closest to *gray value mean*. In the average graphic, plot **C**, the difference is about 4% in the *On* models and 8% in the *Off* models.

As a conclusion, with natural scenes in movement, the similarity is greater when the retina model includes fixational eye movements.

3.2. Static natural scenes

In this experiment we analyze the behavior of the same retina models when they are exposed to a static natural scene. To improve the resolution

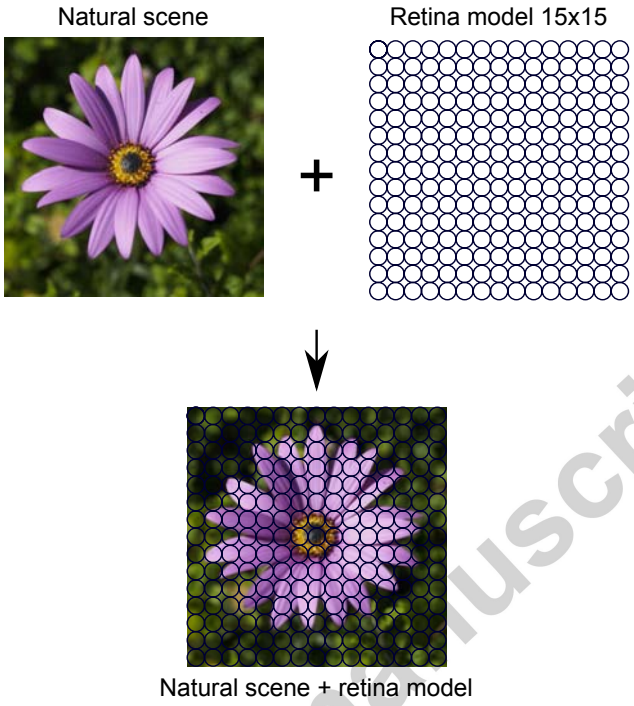

Figure 6: Position of the receptive fields on the image

we have used a matrix of 15×15 ganglionar cells. The exposed image stimulus lasts 60 seconds. This stimulus, showed in Fig. 6, consists in a natural scene image, in this case a flower, with a resolution of 540×540 pixels and 8-bits of color depth. The image covered by the receptive fields is shown in the figure as well. The records were generated in *Neural Events File* format [28] and processed with *Neuroexplorer* [31].

The results of each stimulation are showed in Fig. 7, where the ganglionar cell activity is represented in a 15×15 matrix by means a color code. Each region of this matrix represents the activity of each single ganglion cell. A high activity is represented by light colors and a low activity is represented by dark colors performing a simple reconstruction of the original image. As it can be observed, the On-cells stand out the central area of the image (flower petals), while the Off-cells do the opposite highlighting the contours of petals respect to the background. This behavior is best appreciated in the models having eye movements.

Taking into account these results it is possible to conclude that retina models implementing eye movements are capable to represent better the ob-

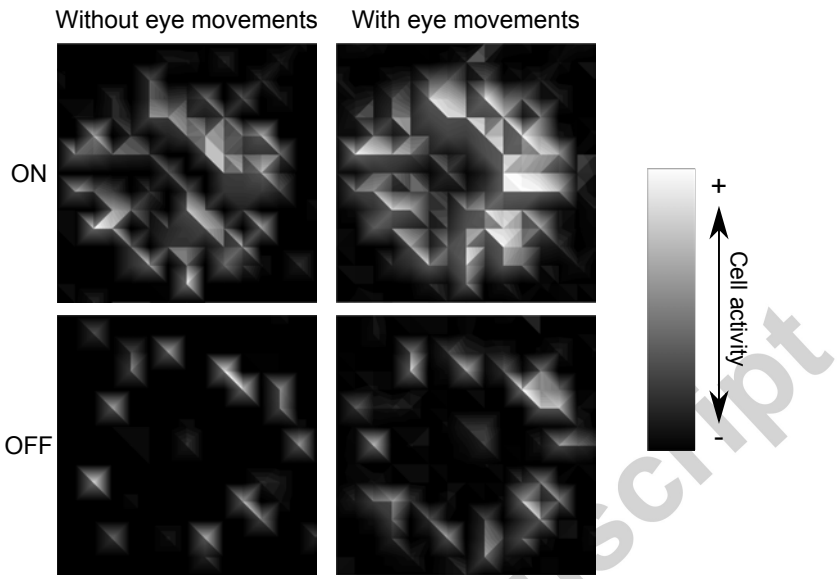

Figure 7: Cell activity graph. White color represents a higher cell response to the stimulus while black color represents a lower cell response.

jects shape, and thus, increasing the activity of cells around the contours where the light undergoes abrupt changes. This behavior can be observed in both On-cells and Off-cells.

In the Fig. 8 the percent of cells activated during stimulation is showed. Owing to the inherent characteristics of the image, there are a greater number of On-cells activated than Off-cells ones. In both cases we find the same pattern, the number of cells activated increases when the retina model implements eye movements.

This behavior occurs because small movements expose each portion of the image to a larger number of cells, which leads to a greater number of excited cells.

4. Conclusions

The role of fixational eye movements in real-world scenes using retina models has been assessed in this paper by means of two experiments. For this purpose the main three types of involuntary eye movements (*tremor*, *drifts*, and *microsaccades*) have been implemented in two ganglionar retina models: *On* model and *Off* model. Results have been compared using the same models without eye movements implemented.

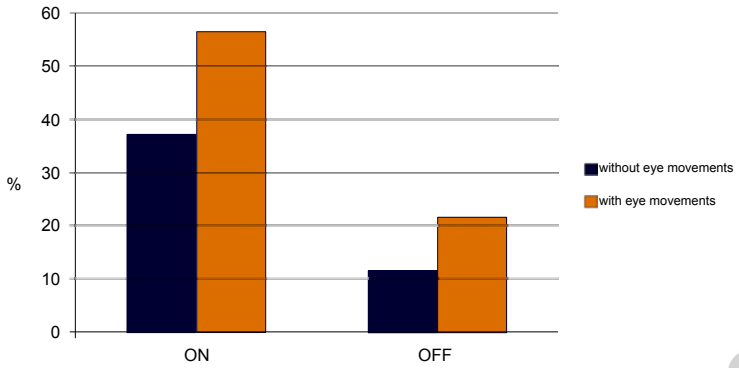

Figure 8: Percent of excited ganglionar cells when stimulated by a static natural scene

In both experiments, the results of this comparison indicate a significant improvement in the visual perception in natural scenes when retina models include *microsaccades*, *tremor* and *drift* movements. Particularly, we observe an increased cellular activity, and a greater number of cells involved in the contour discrimination. Furthermore, neuronal activity records show greater sensitive to light changes, improving the edge recognition. These results indicate that it is possible to improve environment perception if these small movements are incorporated in the retina models and encourage us to implement these eye movements in a future visual neuroprosthesis.

Acknowledgment

This work has been supported in part by the ONCE (National Organization of the Spanish Blind), by the Research Chair on Retinitis Pigmentosa Bidons Egara and by the grant `SAF2008-03694` from the Spanish Government.

[1] S. Martinez-Conde, S. L. Macknik, D. H. Hubel, The Role of Fixational Eye Movements in Visual Perception, Nature Reviews Neuroscience 5 (3) (2004) 229–240. doi:10.1038/nrn1348.
URL `http://dx.doi.org/10.1038/nrn1348`

[2] A. L. Yarbus, Eye Movements and Vision, Plenum. New York., 1967.

[3] F. Ratliff, L. A. Riggs, Involuntary motions of the eye during monocular fixation, Journal of Experimental Psychology 40 (1950) 687–701.

[4] R. Ditchburn, The function of small saccades, Vision research 20 (1980) 271–272. doi:10.1016/0042-6989(80)90112-1.

[5] H. Gerrits, A. Vendrik, Artificial movements of a stabilized image, Vision Research 10 (12) (1970) 1443 – 1456. doi:10.1016/0042-6989(70)90094-5.

[6] J. Krauskopf, Effect of retinal image motion on contrast thresholds for maintained vision, J. Opt. Soc. Am. 47 (8) (1957) 740–741. doi:10.1364/JOSA.47.000740.
URL http://www.opticsinfobase.org/abstract.cfm?URI=josa-47-8-740

[7] C. R. Sharpe, The visibility and fading of thin lines visualized by their controlled movement across the retina, The Journal of Physiology 222 (1) (1972) 113–134. arXiv:http://jp.physoc.org/content/222/1/113.full.pdf+html.
URL http://jp.physoc.org/content/222/1/113.abstract

[8] R. M. Steinman, R. J. Cunitz, G. T. Timberlake, M. Herman, Voluntary control of microsaccades during maintained monocular fixation, Science 155 (3769) (1967) 1577–1579. arXiv:http://www.sciencemag.org/content/155/3769/1577.full.pdf, doi:10.1126/science.155.3769.1577.
URL http://www.sciencemag.org/content/155/3769/1577.abstract

[9] B. Zuber, L. Stark, Saccadic suppression: Elevation of visual threshold associated with saccadic eye movements, Experimental Neurology 16 (1) (1966) 65 – 79. doi:10.1016/0014-4886(66)90087-2.
URL http://www.sciencedirect.com/science/article/pii/0014488666900872

[10] L. Riggs, F. Ratliff, The effects of counteracting the normal movements of the eye, J. Opt. Soc. Am 42 (1952) 872–873.

[11] R. Ditchburn, D. Fender, S. Mayne, Vision with controlled movements of the retinal image, The Journal of physiology 145 (1) (1959) 98–107.

[12] J. Nachmias, Determiners of the drift of the eye during monocular fixation, JOSA 51 (7) (1961) 761–766.

[13] M. Greschner, M. Bongard, P. Rujan, J. Ammermüller, et al., Retinal ganglion cell synchronization by fixational eye movements improves feature estimation, Nature neuroscience 5 (4) (2002) 341–347.

[14] K. Donner, S. Hemilä, Modelling the effect of microsaccades on retinal responses to stationary contrast patterns, Vision research 47 (9) (2007) 1166–1177.

[15] A. Wohrer, P. Kornprobst, Virtual retina: A biological retina model and simulator, with contrast gain control, Journal of Computational Neuroscience 26 (2009) 219–249.

[16] A. Martínez, L. Reyneri, F. Pelayo, S. Romero, C. Morillas, B. Pino, Automatic generation of bio-inspired retina-like processing hardware, Computational Intelligence and Bioinspired Systems (2005) 461–465.

[17] M. Bongard, J. M. Ferrandez, E. Fernandez, The neural concert of vision, Neurocomputing 72 (4-6) (2009) 814–819. doi:10.1016/j.neucom.2008.06.022.

[18] A. Martínez-Álvarez, A. Olmedo-Payá, S. Cuenca-Asensi, J. Ferrández, E. Fernández, Retinastudio: A bioinspired framework to encode visual information, Neurocomputing.

[19] C. Morillas, S. Romero, A. Martínez, F. Pelayo, E. Fernández, A computational tool to test neuromorphic encoding schemes for visual neuroprostheses, Lecture Notes in Computer Science. Computational Intelligence and Bioinspired Systems 3512 (2005) 268–316.

[20] W. Gerstner, W. M. Kistler, Spiking Neuron Models: Single Neurons, Populations, Plasticity, Cambridge University Press, 2002.

[21] J. L. Gauthier, G. D. Field, A. Sher, M. Greschner, J. Shlens, A. M. Litke, E. J. Chichilnisky, Receptive fields in primate retina are coordinated to sample visual space more uniformly, PLoS Biol 7 (4) (2009) e1000063.

[22] R. Carpenter, Movements of the eyes pion (1988).

[23] E. Stacy, A generalization of the gamma distribution, The Annals of Mathematical Statistics 33 (3) (1962) 1187–1192.

[24] R. M. Pritchard, Stabilized images on the retina, WH Freeman Company, 1961.

[25] J. Ferrández, M. Bongard, F. García de Quirós, J. Bolea, J. Ammermü, R. Normann, E. Fernández, Decoding the population responses of retinal ganglions cells using information theory, Connectionist Models of Neurons, Learning Processes, and Artificial Intelligence (2001) 55–62.

[26] R. A. Normann, E. M. Maynard, P. J. Rousche, D. J. Warren, A neural interface for a cortical vision prosthesis, Vision Research 39 (15) (1999) 2577 – 2587. doi:http://dx.doi.org/10.1016/S0042-6989(99)00040-1.
URL http://www.sciencedirect.com/science/article/pii/S0042698999000401

[27] A. D. Straw, Vision egg: an open-source library for real-time visual stimulus generation., Frontiers in neuroinformatics 2. doi:10.3389/neuro.11.004.2008.
URL http://dx.doi.org/10.3389/neuro.11.004.2008

[28] Neural Event Format, http://cyberkineticsinc.com/NEVspc20.pdf, [Online; accessed 12-May-2011] (2008).

[29] *NeurALC*, http://neuralc.sourceforge.net, [Online; accessed 23-Nov-2011] (2006).

[30] M. Mancuso, R. Poiuzzi, G. Rizzotto, A fuzzy filter for dynamic range reduction and contrast enhancement, in: Fuzzy Systems, 1994. IEEE World Congress on Computational Intelligence., Proceedings of the Third IEEE Conference on, IEEE, 1994, pp. 264a–a264d.

[31] *Neuroexplorer*, http://www.neuroexplorer.com, [Online; accessed 03-Jan-2014] (2006).